Silicon Micromachined Sensor for Broadband Vibration Analysis

Adolfo Gutiérrez, Daniel Edmans, Chris Cormeau, Gernot Seidler
InterScience, Inc.
Troy, NY 12180

and

Dave Deangelis†, Edward Maby††
†Department of Mechanical Engineering
††Department of Electrical, Computer and Systems Engineering
Rensselaer Polytechnic Institute
Troy, NY 12180-3590

SBIR Sponsors: DoD AF, DoD ARMY-ARPA

ABSTRACT

The development of a family of silicon based integrated vibration sensors capable of sensing mechanical resonances over a broad range of frequencies with minimal signal processing requirements is presented. Two basic general embodiments of the concept were designed and fabricated. The first design was structured around an array of cantilever beams and fabricated using the ARPA sponsored MUMPS process at MCNC. As part of the design process for this first sensor, a comprehensive finite elements analysis of the resonant modes and stress distribution was performed using PATRAN. Dependence of strain distribution and resonant frequency response as a function of Young's Modulus in the Poly-Si structural material was studied. Analytical models were also studied. In-house experimental characterization using optical interferometry techniques were performed under controlled low pressure conditions. A second design, intended to operate in non-resonant mode and capable of broadband frequency response, was proposed and developed around the concept of a cantilever beam integrated with a feedback control loop to produce a null mode vibration sensor. A proprietary process was used to integrate a MOS sensing device, with actuators and a cantilever beam, as part of a compatible process. Both devices, once incorporated as part of mutifunction data acquisition and telemetry systems will constitute a useful system for NASA launch vibration monitoring operations. Satellites and other space structures can benefit from the sensor for mechanical condition monitoring functions.

INTRODUCTION

Over the past 10 years the research and development efforts aimed towards producing very small electromechanical components using microelectronics fabrication techniques have received ever increasing attention. As a result of these efforts, various competing technologies have emerged as leading contenders. In Europe, high aspect ratio microstructures fabricated using the LIGA (Lithographie, Galvanoformung und Abformung) process based on the use of thick photoresist, synchrotron based x-ray lithography and injection molding has become dominant. Japan, driven by MITI coordinating efforts, has chosen to miniaturize components through mechanical microfabrication using high precision machinery. In the United States the most developed technology for the fabrication of micromachined devices relies on using silicon bulk or surface micromachining.

A typical silicon surface micromachining process begins with a silicon wafer upon which alternating layers of structural (Poly-Si) and sacrificial material (SiO_2) are deposited and selectively etched to produce structures that have relatively small aspect ratios. The thickness of the depositions is limited to a few microns because of photoresist thickness and etch rate limitations, and because of built-

in or intrinsic residual stresses that tend to increase as the thickness of the layers increases. These process created stresses can only be partially relieved through thermal annealing and the remaining residual stress can determine severe structural deformations after final chemical release.

Although silicon micromachining of Micro-Electromechanical Systems (MEMS) has rapidly become a major research area, only a handful of successful commercial devices have been produced. The consolidation of MEMS devices as a segment of the sensors and microelectronics industry ultimately will rely on proper product definition, skillful market identification, and competitive cost-benefit ratios. InterScience, Inc. has decided to focus its research and development efforts in a group of relatively simple integrated mechanical vibration sensors suitable for real time vibration analysis of mechanical structures. These types of sensors would have applications in transportation and other mechanical systems where reliability if of utmost concern. Systems such as launch and orbital vehicles, permanent space structures, aircrafts and missiles are examples of such systems of direct interest to NASA, FAA and DoD. Also, high reliability mechanical systems are found throughout the nuclear cycle. Some potentially mass producible applications, such as engine analysis in the ground and sea transportation industries, are also readily conceivable. Cost-benefit tradeoffs will ultimately be the determining factor in the commercial success of these types of sensors.

Earlier work by Benecke and Csepregi[1] demonstrated the feasibility of building resonant vibration sensors using a piezoelectric sensor located at the base of the cantilever beams, where the strain is maximum. Additional work by Motamedi[2] from Rockwell demonstrated cantilever based accelerometers fabricated in silicon using piezoelectric capacitive sensors and a PMOS amplifier, in a process fully VLSI compatible. Both sensors exhibited narrow band responses that could potentially be improved through the use of feedback control schemes. Inspired by these initial investigations, our team decided to pursue the development of a family of vibration sensors, both resonant and non-resonant, using silicon surface micromachining[3]. The goal of the first effort was to develop a resonant vibration sensor capable of real time spectral analysis using an array of cantilever beams. The goal of the second related effort was to produce a wideband vibration sensor incorporating feedback control and integrated capacitive position sensing.

This paper describes the various aspects that we have encountered in the development of our vibration sensors. Critical proprietary information has been left out of the discussion. The development is still an ongoing effort implying that some critical information for performance assessment is missing. The paper starts with a review of the effort of producing an array of resonant piezoresistive vibration sensors. It follows with a review of the fabrication process which was used by MCNC in our first design. Numerical analysis of our sensors, based on finite element methods is then surveyed. It follows a discussion of the rationale for incorporating feedback forced balance schemes. Finally a discussion of our in-house mechanical characterization capabilities based on interferometry is presented.

SILICON MICROMACHINED RESONANT VIBRATION SENSOR

A number of functional prototypes were fabricated using the MCNC (formerly Microelectronics Center of North Carolina) foundry as part of the MUMPS4 (Multi-User MEMS Process, Run # 4). This multiproject process is supported by ARPA as part of a multi-year infrastructure program for MEMS development. Figure 1 is a general cross section of the two-layer polysilicon surface micromachining MUMPs process[4]. This process has the general features of a standard surface micromachining process: (1) polysilicon is used as the structural material, (2) deposited oxide is used as the sacrificial layer, and (3) silicon nitride is used as electrical isolation between the polysilicon and the substrate.

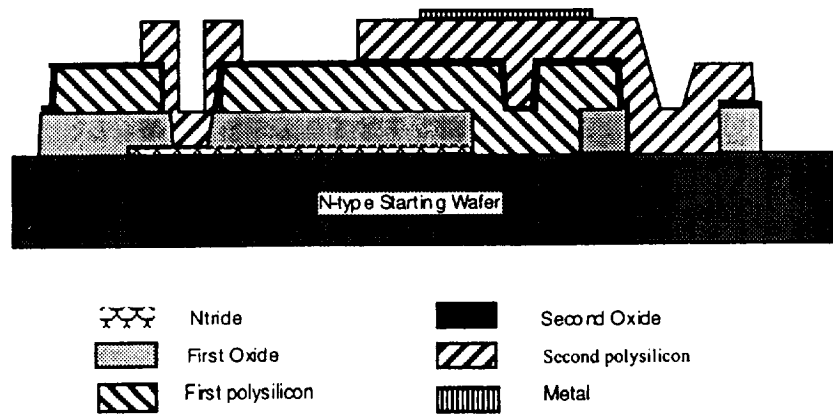|			
Nitride		Second Oxide	
First Oxide		Second polysilicon	
First polysilicon		Metal	

Fig. 1   Double-layer Poly-Silicon MUMPS process (not to scale)

The MUMPS fabrication process begins with n-type <100> 100 mm silicon wafers. Next, a 500nm thick low stress silicon nitride layer is deposited on the wafers as an electrical isolation layer, followed by a thin layer of electrical polysilicon deposited to allow the user to design an electrical sensing or electrode plate, isolated from the wafer, below the first mechanical polysilicon layer. It is followed by a 2.0 µm thick first oxide sacrificial layer. This layer of oxide is will be removed at the end of the process to free the first mechanical layer of polysilicon. Next, the first structural layer of polysilicon is deposited. The thickness of the polysilicon layer is 2.0 µm. A thin masking layer of second oxide is deposited. After the first layer of polysilicon is patterned, a second sacrificial thin oxide layer is deposited. This oxide layer will be removed at the end of the process to facilitate the release of the second mechanical polysilicon layer. Next, the second 1.5 µm thick polysilicon layer is deposited. As with the first polysilicon layer, a thin sacrificial oxide layer is deposited as an etch mask and dopant source. The final deposited layer in the MUMPs process is a 1.0 µm thick aluminum layer. The front side of the wafer is protected and the polysilicon and oxide layer on the back of the wafer are removed by wet chemical etching. The nitride layer is left on the back of the wafer in case post-processing of the die is desired at the MUMPS participants own facility.

Each of the dies fabricated using MUMPS4 contained an array of resonators. The typical resonator consisted of a cantilever beam that has an additional loading mass of deposited aluminum placed on the free end to reduce the resonant frequency. It could also have a piezoelectric material deposited at the base that acts as a strain gauge. A depiction of the 1 cm^2 die fabricated is shown in Figure 2. An schematic representing the basic concept is shown on Figure 3.
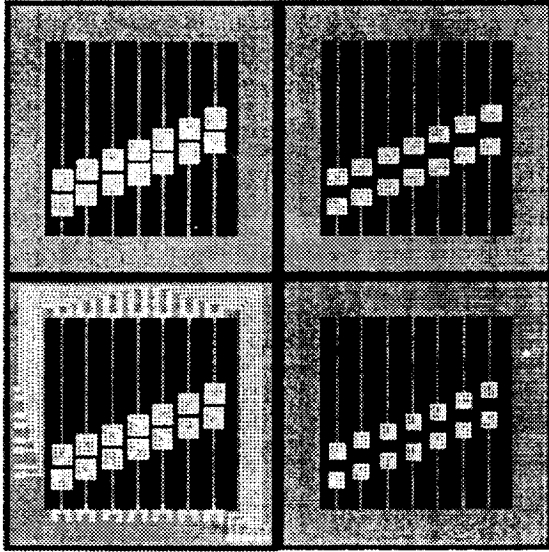
Figure 3. Cantilevered beam showing placement of piezoresistor and loading mass.

Figure 2. A 1 cm^2 die containing the first four cantilever test structures fabricated using MUMPS 4.
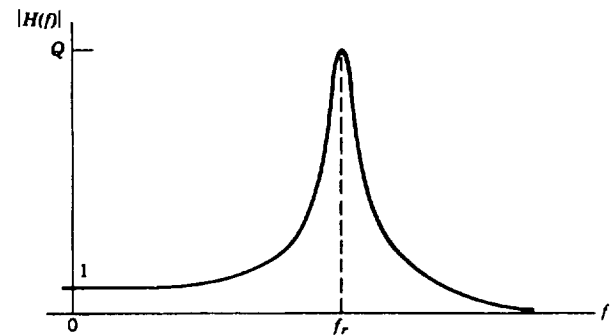

Figure 4. Transfer function of a single cantilever beam oscillator.

The resonant frequency of the beam is a function of several parameters including Young's Modulus of elasticity, the beam length, the thickness of the beam, the density of the polysilicon, and the density of the surrounding media. A typical transfer function is shown in Figure 4. The selectivity is represented by the peak at the resonant frequency, f_r, and it is characterized by the width at half maximum power (FWHM), which is strongly dependent on the geometry of the end mass and the viscosity of the surrounding gas or fluid. For the particular designs implemented, the width of the resonant peak is about 1 Hz in vacuum and 800 Hz in air at STP. The selectivity and sensitivity are trade-offs that have to be made to provide the right combination for the particular application. The strain is related to the driving acceleration and the physical parameters of the beam. The maximum acceleration that the beam can sustain is given by substituting the maximum yield strength for silicon of $10^{-3}N/m^2$ into the strain equation. The resulting value is in the thousands of g's range for our design. A variable resistance directly proportional to the strain is developed in the piezoelectric crystal. It is also proportional to the piezoelectric material's coupling coefficient, and the area of the piezoelectric deposition, and inversely proportional to the combination of the capacitance of the piezoelectric material and parasitic capacitances.

FINITE ELEMENT ANALYSIS

The critical aspect of the design is the resonant frequency and the mechanical quality factor, Q, of each cantilever beam. An advantage of a micro-machined vibration sensor, in addition to its small size and potential for low cost fabrication, is the ability to provide high sensitivity to a discrete set of vibrational frequencies.

In order to accurately predict the response of the beams to the driving forces, it is necessary to perform finite element analysis calculations. The use of finite element analysis also provides estimates for the strain induced at the anchored end of each beam. The strain distribution thus calculated is used

to predict the optimum location for the piezoelectric material in order to maximize the charge that will accumulate in the piezoelectric material, which is directly related to the output piezo-voltage to be measured.

Initially, the numerical analysis was carried out using the commercial software package for finite element analysis, PATRAN. The analysis of the shortest cantilever beam in the array, measuring 380 μm to the inside edge of a 300 μm square paddle. Based on the finite element analysis performed, the resonant frequency of the beams vary from 220 Hz to 2,245 Hz. It is important to be aware that the FEA models rely on *a priori* knowledge of the Young's Modulus, a parameter that for the case of Poly-Si, varies significantly for each specific fabrication process. More recently we have centered our numerical analysis work around the FEA package WECAN.

The fundamental frequency of the beams depicted in this section is much higher than will be designed and is only being used for illustrative purposes. Figure 5 shows the stress distribution in a beam that has a paddle on the free end. The paddle reduces the resonant frequency and broadens the resonant peak. This shows the use of the FEA, to identify areas of high stress during the design process in order to alleviate any problems by careful early planning.
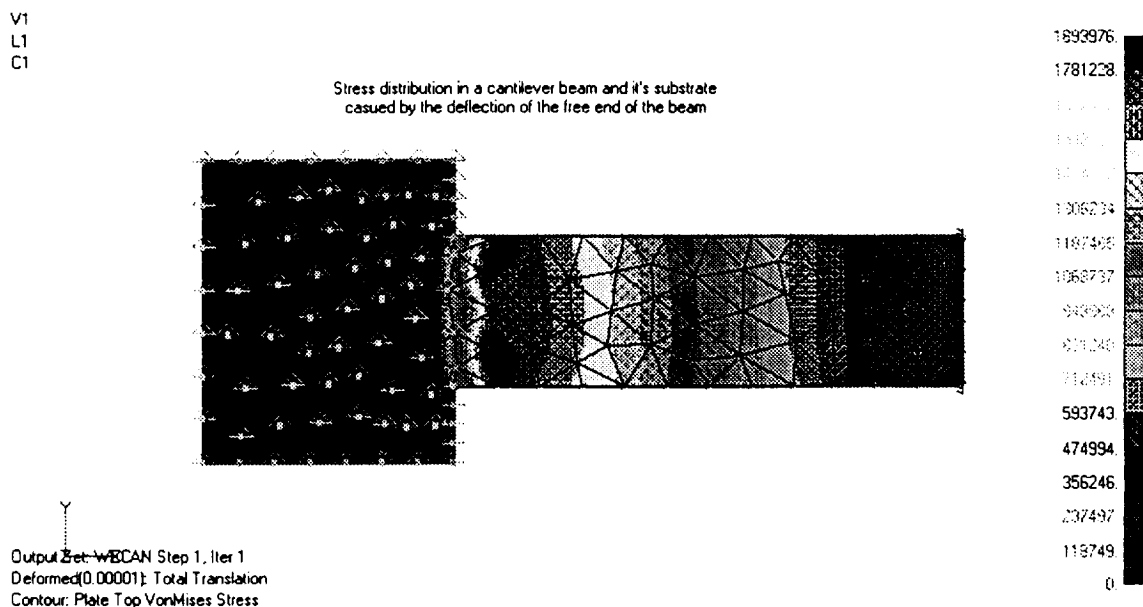

Figure 5. Stress distribution in a typical beam showing the highest stress concentration at the constrained end.

For a structure which is 1.5 μm thick, 60 μm wide and 200 μm long, the fundamental mode, shown in Figure 7, occurs at 50,859 Hz and the typical deflection is 144 μm when it is not constrained. The stress distribution is represented by the shading. The shape of the deflection is important because the capacitance will vary as the beam is deflected. At higher modes 3 and 5 the beam twists. The next four frames in Figure 8 show the shape the beam takes in each of the first four higher order modes, numbers 2 through 5.
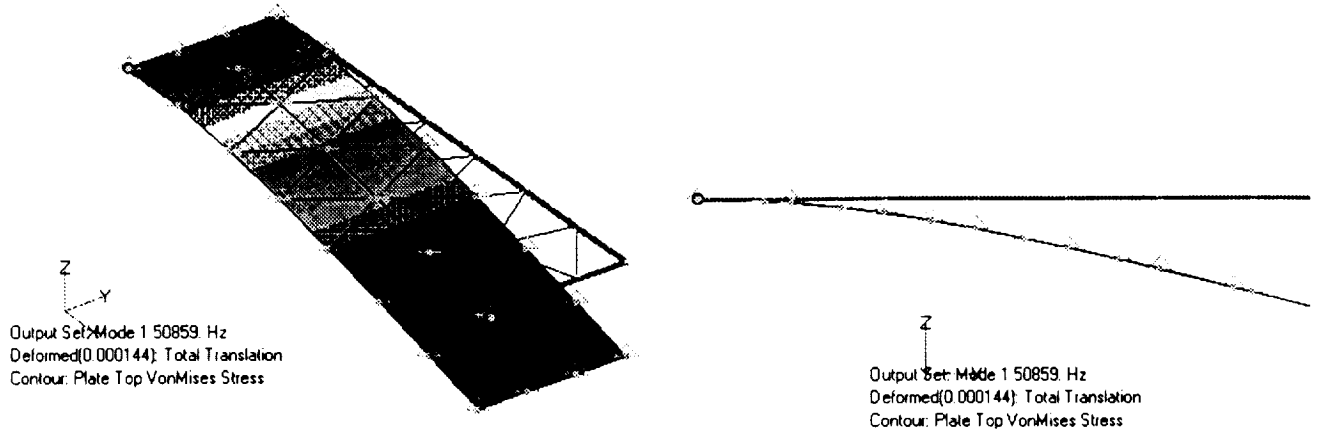
Output Set>Mode 1 50859. Hz
Deformed(0.000144): Total Translation
Contour: Plate Top VonMises Stress

Output Set: Mode 1 50859. Hz
Deformed(0.000144): Total Translation
Contour: Plate Top VonMises Stress

Figure 7. The shape of a simple beam in the fundamental mode.

Output Set>Mode 2 317520. Hz
Deformed(0.0000503): Total Translation
Contour: Plate Top VonMises Stress

Output Set>Mode 3 346090. Hz
Deformed(0.0000338): Total Translation
Contour: Plate Top VonMises Stress

Output Set>Mode 4 902870. Hz
Deformed(0.0000257): Total Translation
Contour: Plate Top VonMises Stress

Output Set>Mode 5 1100100. Hz
Deformed(0.0000313): Total Translation
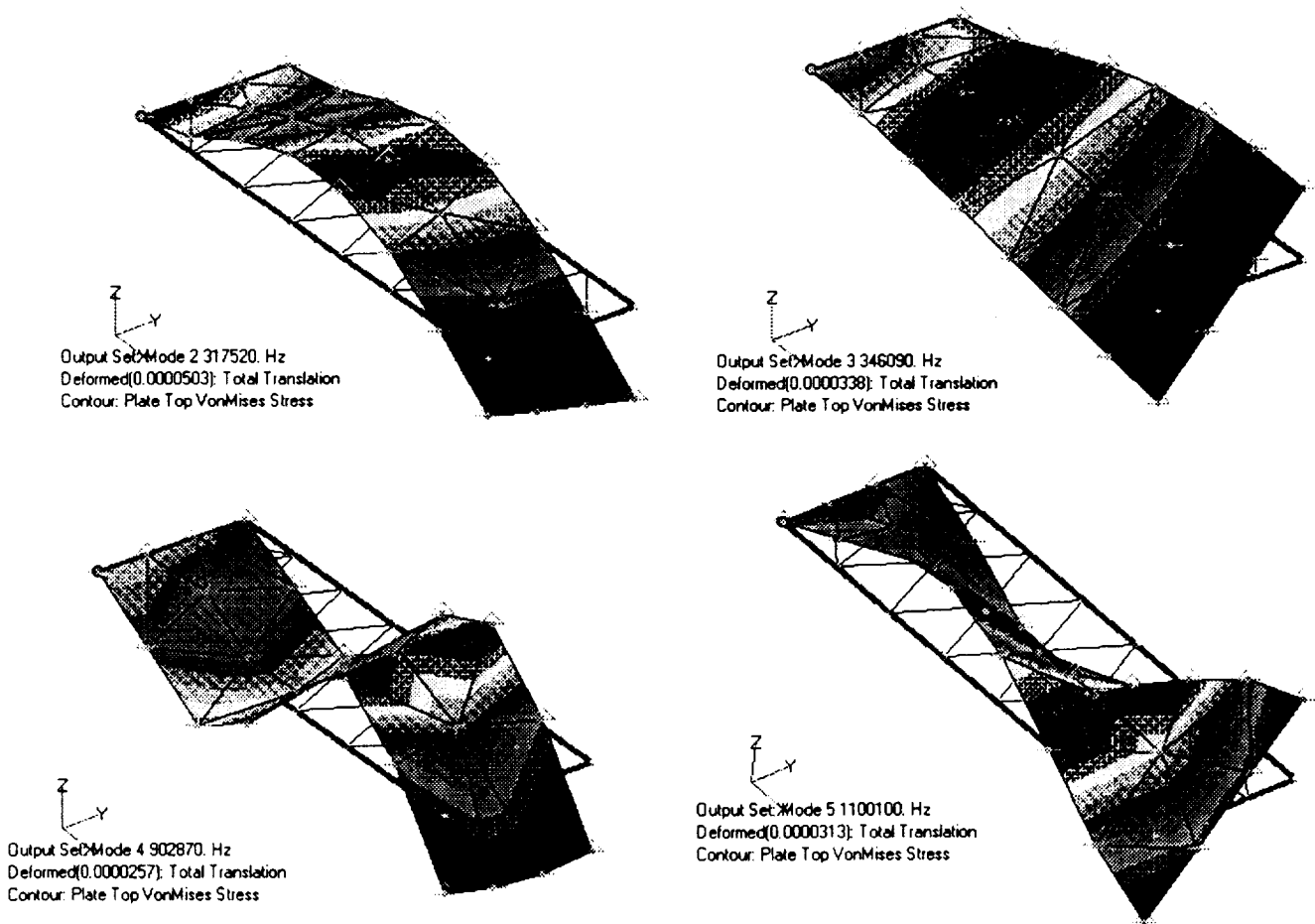Contour: Plate Top VonMises Stress

Figure 8 The first four higher order modes, 2-5, of a typical beam showing the shape and the scaled deflection. The strain distribution is represented by the shading.

The comparison of the normalized deflections shown in the preceding pictures shows that the maximum displacement associated with the higher order modes is always less than 30% of the displacement of the beam in its fundamental mode. Figure 9 below shows the relative displacement of the beam in each of the first five modes relative to the sixth mode. It shows that there is very little deflection associated with the higher modes, although it cannot be ignored.
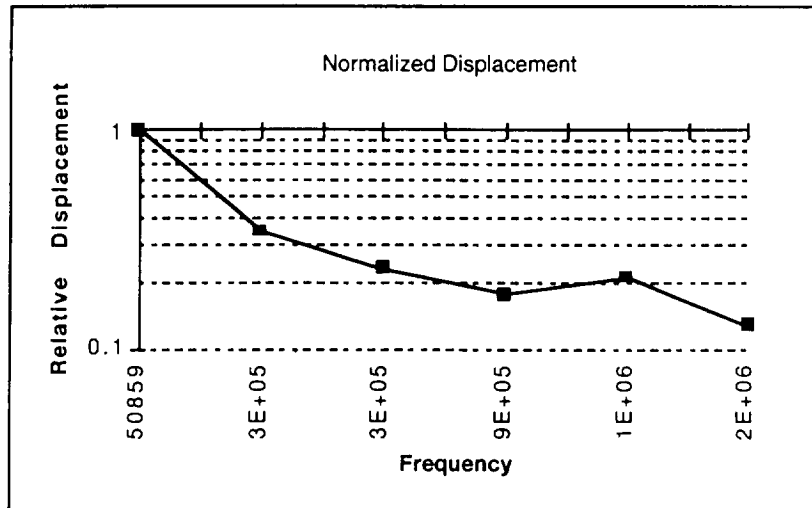
Figure 9 Relative deflection of the beam in each of the first six modes.

The resonant vibration sensor was determined to be adequate for applications in which *a priori* knowledge of the mechanical frequencies is available. Although in principle it is possible to cover a large spectral range through the use of a very large number of cantilever beams, in practice however, this approach will result in large and highly redundant devices, implying high unit cost. Furthermore, resonant devices impose severe packaging restrictions since they require vacuum sealed operation to reduce viscous damping.

A concept that has been used for several decades in the field of seismology is the null mode forced balance feedback operation of an inertial vibration sensor which improves all the mechanical performance figures. It enables wider broadband, higher sensitivity and simplified packaging requirements.

SILICON MICROMACHINED WIDEBAND NON-RESONANT VIBRATION SENSOR

The force-balance vibration sensor derives its name from the forces applied electrostatically between its suspended mass and frame through the use of a feedback loop. Two forces are involved, one variable force proportional to the displacement of the mass relative to the frame that tends to balance this displacement and so behaves as a variable spring, a second force is proportional to the relative velocity and provides lossless dynamic damping.
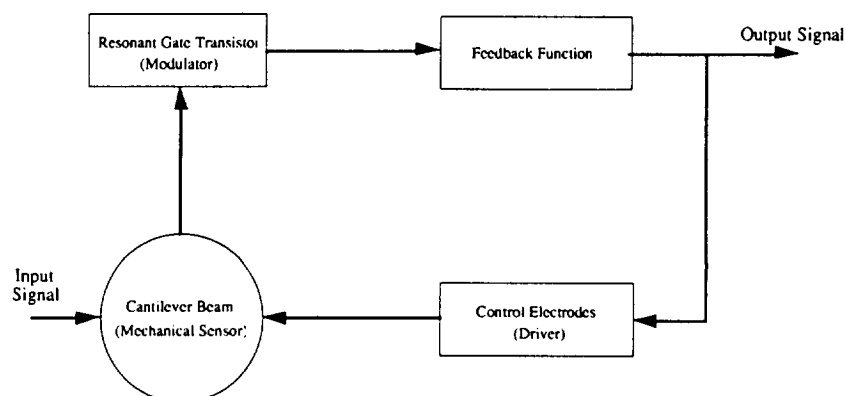

Figure 10. Force-balance feedback control block diagram.

The fundamental equation describing any inertial vibration sensor is[5]:

$$\frac{d^2x_r}{dt^2} + \frac{R}{M}\frac{dx_r}{dt} + \frac{1}{MC}x_r = \frac{d^2x_i}{dt^2}$$

where M is the suspended mass, x_i is the external mechanical excitation, R is the viscous damping resistance and C is the compliance of the supporting spring.
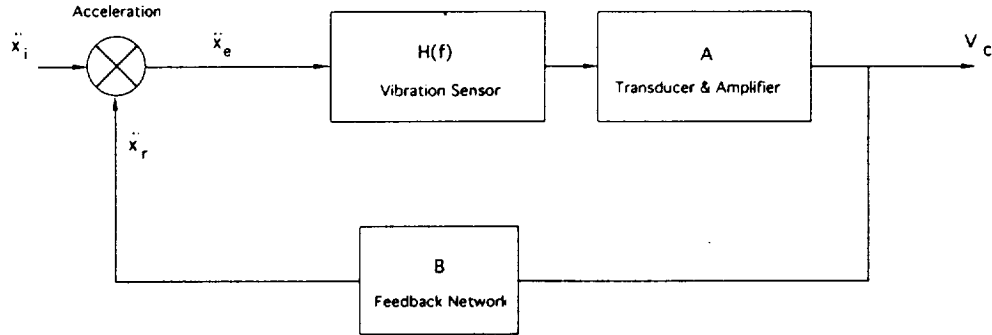

Figure 11. Force-balance feedback control diagram

The application of negative force-feedback to a seismometer produces a number of advantages and is in fact essential when a small mass is suspended with a high Q, in order to achieve a satisfactory transient response. The most useful form of feedback is negative displacement, which tends to keep the mass fixed in a position with respect to its support, making the suspension appear more stiff and increasing the natural frequency.

The transfer function of the vibration sensor represented in Fig. 11 is :

$$\frac{x_r}{\ddot{x}_i} = \frac{1}{s^2 + 2\xi\omega_0 s + \omega_0^2}$$

$s=jw$ is the Laplace operator and ξ is the damping ratio. The closed-loop transfer function is

$$\frac{v_0}{\ddot{x}_1} = \frac{A}{s^2 + 2\varepsilon\omega_0 s + \omega_0^2}$$

where v_0 is the output voltage, A is the gain in the forward path and B is the transfer function of the feedback path, and becomes $1/B$ when AB is the dominant term. If it is assumed that AB is independent of frequency, the DC loop gain L is $(1/\omega_0^2)AB$ and the natural frequency is increased by a factor $L^{1/2}$, the damping being reduced by the same factor. The response is essentially flat (to acceleration) from DC to the new natural frequency and the transient response can be controlled by a compensation network in the feedback path.

The fundamental limit of detection of any vibration sensor is determined by the Brownian motion of the mass. It has been shown that the noise equivalent acceleration (d^2x_i /dt^2) for a bandwidth f is given by

$$(x)_{ne}^2 = \frac{4RkT\Delta f}{M^2} = \frac{4kT}{M}\frac{\omega_o}{Q}$$

where kT is the equi-partition energy and Q is the quality factor of the suspension. It can be observed that a small mass may be used provided that the damping is low. A typical micromachined device, such as the one we have developed has a mass of about 0.3 µg; Q of about 1000, and a natural frequency of a 1kHz which determines that the noise equivalent acceleration is about 3.5 x 10^{-13} m^{2}s^{-3}. In fact this

device is extremely sensitive, thus Brownian noise will not be important and the electronic noise, mainly thermal, will ultimately determine the sensitivity of the micro seismometer.

Mechanical design requirements are eased and the desired wideband response is simply determined by the feedback parameters. The signal-to-noise is unaffected by feedback. The response is controlled by applying forces to the mass; this does not affect the Brownian motion, whereas adding damping to control the response in an open loop-system increases the dissipation and therefore increases the Brownian motion. Furthermore, it is easy to verify that a very small mass can be suspended with a high Q and employed in a feedback system of suitable loop gain, can thus provide a flat response and adequate detectivity over the whole range of interest in seismology. Additionally advantages, over conventional open-loop instruments are obtained in linearity, dynamic range and calibration.

In the control loop shown in Figure 10, two electronic transducers are attached to the sensor, one being the modulator, in our case our proprietary capacitive sensing device, and the other being a driver or control electrodes to provide mechanical force opposing the displacement. The cross section of a device currently being fabricated that implements this closed feedback control loop is shown in Figure 12. It can be observed in the cross-sectional view that two control electrodes have been inserted. The sensing element of the loop is a proprietary capacitance measuring device.
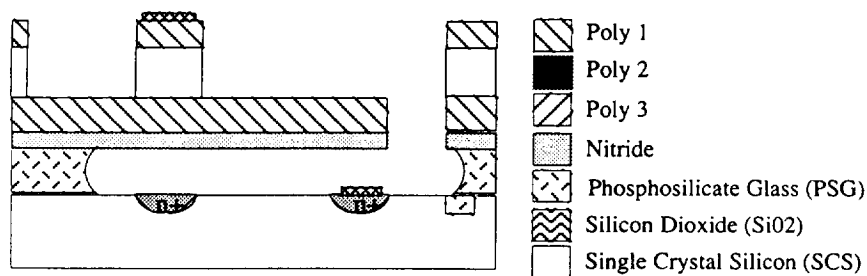

	Poly 1
	Poly 2
	Poly 3
	Nitride
	Phosphosilicate Glass (PSG)
	Silicon Dioxide (SiO2)
	Single Crystal Silicon (SCS)

Figure 12 Cross-sectional view of the Silicon Micromachined Wideband Vibration Sensor.

EXPERIMENTAL CHARACTERIZATION USING OPTICAL INTERFEROMETRY TECHNIQUES

Following fabrication of a vibration sensor die, they must be tested and characterized. This is accomplished by using an interferometric technique developed in our own laboratories. A diagram of the optical test set-up used to characterize the frequency response of the resonators is shown in Figure 13. A Fabry-Perot (FP) type interferometer is to be used to measure very small deflections of the cantilever beam. In general an FP interferometer contains two plates separated by a gap. In the case of the FP interferometer used here, the first plane is a partial reflector, formed by the end surface of the fiber. The total reflector is the silicon target. Provided that the resonator is moving, the standoff distance will change producing a changing interference pattern. The fringe pattern can be resolved using our system to an accuracy of $\lambda/30$ or up to ±27 nm for an 820 nm wavelength source.
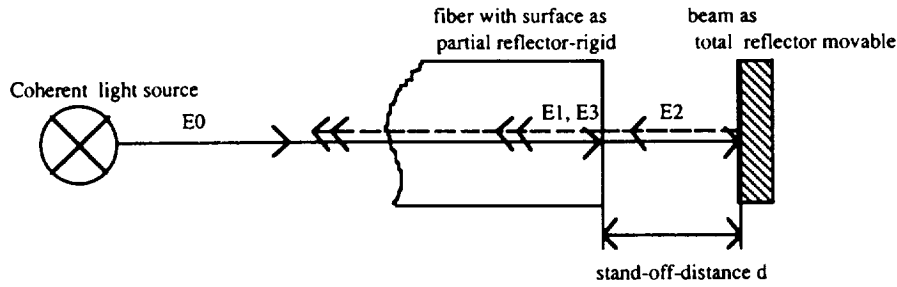
Figure 13. Fabry-Perot-Interferometer based on single mode fiber interface.

The fringe visibility is given as

$$\alpha = \frac{I_{max} - I_{min}}{I_{max} + I_{min}}$$

where I_{max} and I_{min} are the relative maxima and minima of the intensity in the range of $d \pm \Delta d$. The deflection of the beam, which is variation of the stand-off distance, will change with the applied voltage. The resulting optical phase difference varies linearly. The optical phase difference $\phi(t)$ corresponds to

$$\phi(t) = \frac{4\pi}{\lambda} d(t)$$

where $d(t)$ is deflection of the beam and λ is the wavelength of the light source.

The beam is deflected with the application of a modulation current through the electrode. A variety of deflection waveforms can be used to characterize the material parameters and the response of the beam. A moving beam will modulate the frequency of the interferometric signal. In addition, a reference signal is needed to differentiate the motion of the vibrating beam from any residual motion of the surrounding support structure. The reference signal is achieved by a second interferometer that is pointed to the die substrate. Figure 14 shows the setup of the measurement system.
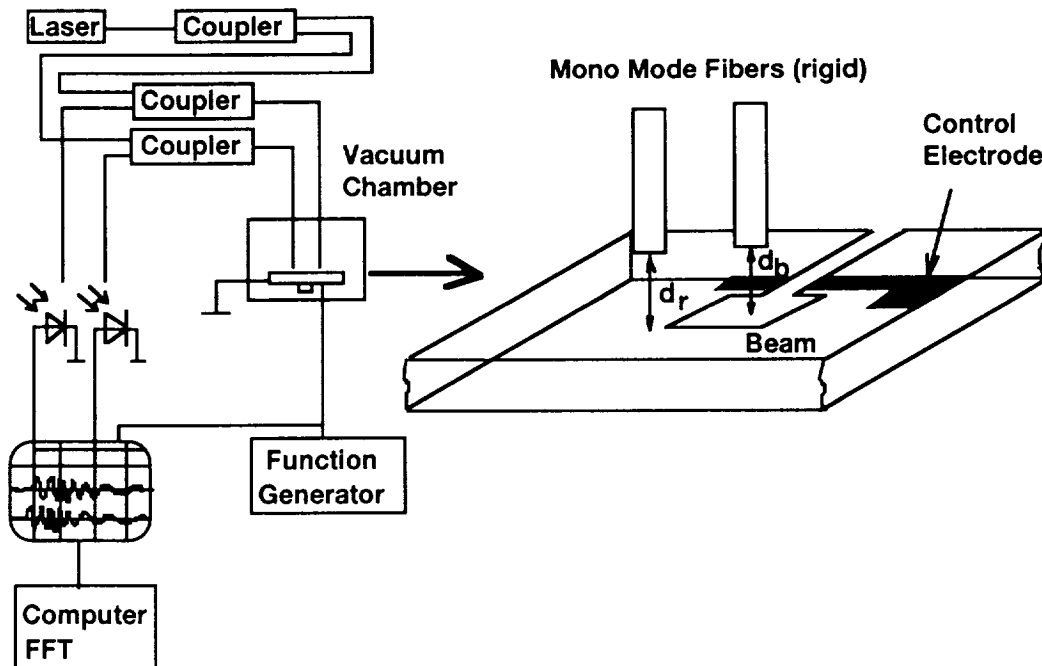

Figure 14. Setup for measuring the movement of the beams.

As mentioned above, the data resulting from this interferometric system is acquired using LabView. This software package is used to both control laboratory equipment and to analyze the resulting measurements through the use of virtual instruments. However, an illustrative example is included below. First data is collected and processed to show the magnitude and phase of the signal. This data is consequently processed to determine the spectral content. The information in the frequency domain will include the fundamental frequency as well as a beat frequency generated from the mixing that occurs due to the nature of the interferometric system. This beat frequency comes from the convolution of the two signals, one is the reference and the other is the beam itself. Figure 15 shows the results of the analysis with the spectral content of the beam response clearly shown.
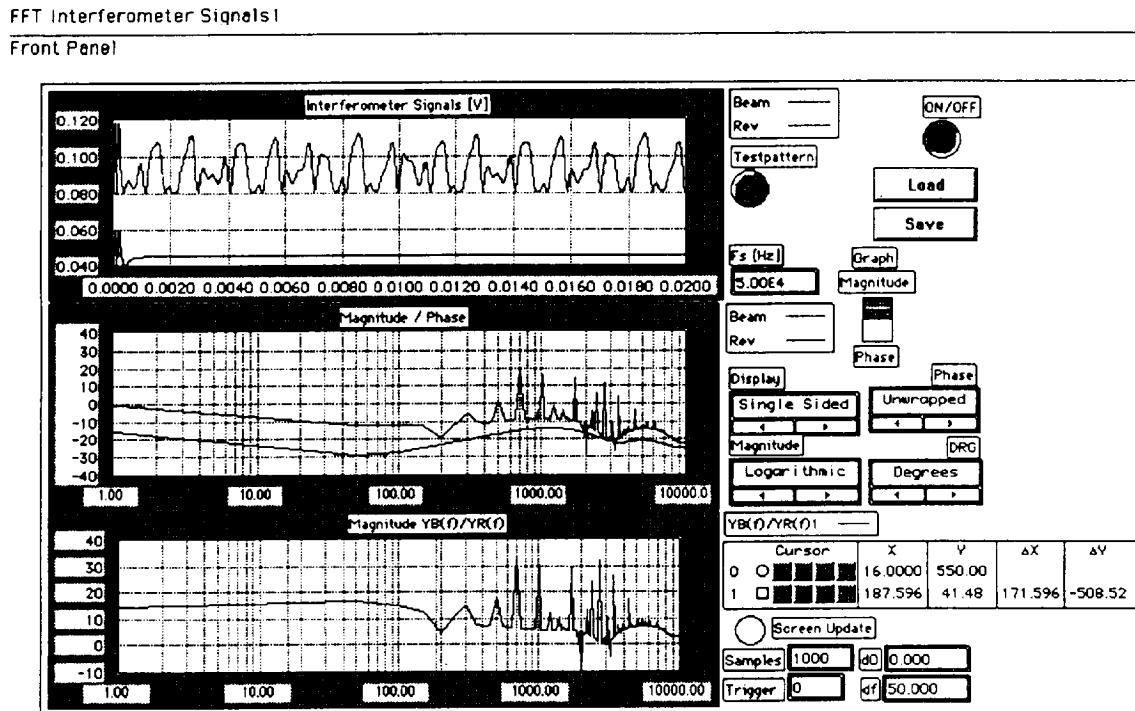

Figure 15. Results screen of virtual instrument showing the spectrum producedfrom the Fourier Transform and the impulse response of the beams.

CONCLUSIONS

The evolutionary development of a micromechanical vibration sensor has been described Starting from a preliminary concept implemented using the ARPA sponsored MUMPS at MCNC, the fabrication and characterization of a number of resonant vibration sensor was carried out. During characterization of this type of sensor, it was determined that viscous damping imposes severe limitations on the performance of the simple resonators indicating the need for vacuum sealed encapsulation of the devices.

Finite element modeling efforts were able to provide qualitative information. The fact that the Young's Modulus for Poly-Si can assume a wide range of values requiring experimental determination for each particular process, reduces the quantitative potential of the FEA in earlier design stages.

The use of a closed feedback control loop in a configuration known as force balanced vibration sensor, has the advantage of enabling broadband operation thus simplifying the number of cantilever sensors required at expense of higher processing complexities. At present we are still carrying out the various fabrication steps and currently this second set of devices is awaiting final processing.

Metrological characterization of the devices has been implemented using a fiber optic interferometric technique developed at InterScience that has been succesfully applied for directly measuring deflection and frequency response of cantilever type vibration sensors.

1 W. Benecke, L. Csepregui et al, "A frequency selective, piezoresistive silicon vibration sensor", 3rd International Conference on Solid-State Sensors and Actuators, 1985, pp. 105-108.

2 M.E. Motamedi, et al., " Application of electrochemical etch-stop in processing silicon accelerometer", Proc. 1982 Electrochemical Society Meeting, May 9-14, p 188.

3 DoD sponsored both efforts under USAF contract #F29601-94-C-0095 and under ARPA/BMDO contract number DASG60-94-C-0081.

4 D. Koester, R. Mahadevan and K. Markus, "MUMPs: Introduction and Design Rules", Rev. 3, MCNC, Oct. 1994

5 M.J. Usher et al., "A miniature wideband horizontal-component feedback seismometer", Journal of Physics E: Scientific Instruments 1977 Vol. 10